



# Optical coherence tomography retinal imaging: narrative review of technological advancements and clinical applications

Christopher S. Langlo, Aana Amin, Susanna S. Park<sup>^</sup>

Department of Ophthalmology & Vision Science, University of California Davis, Sacramento, CA, USA

**Contributions:** (I) Conception and design: CS Langlo, SS Park; (II) Administrative support: SS Park; (III) Provision of study materials or patients: CS Langlo, SS Park; (IV) Collection and assembly of data: All authors; (V) Data analysis and interpretation: All authors; (VI) Manuscript writing: All authors; (VIII) Final approval of manuscript: All authors.

**Correspondence to:** Susanna S. Park, MD, PhD. Department of Ophthalmology & Vision Science, University of California Davis, Ernest E. Tschannen Eye Institute, 4860 Y St., Sacramento, CA 95817, USA. Email: sspark@ucdavis.edu.

**Background and Objective:** Optical coherence tomography (OCT) is a non-invasive imaging tool that can provide rapid cross-sectional images of the retina, cornea, and optic nerve head in live patients. The objective of this review is to provide an overview of the technical advancements and current clinical applications of OCT for managing patients with retinal disorders.

**Methods:** Narrative overview synthesizing the findings of literature retrieved from searches of computerized database, authoritative texts and authors' clinical experience and expertise.

**Key Content and Findings:** Unlike the first-generation time-domain OCT (TD-OCT) instruments, the newer spectral-domain OCT (SD-OCT) instruments use a broadband light source to increase axial image resolution. In addition, the decreased image acquisition time also increases the transverse image resolution, reduces motion artifacts, and allows serial cross-sectional images of the retina to be obtained rapidly. A three-dimensional (3D) image of the retina, reconstructed using serial two-dimensional (2D) OCT images, can be used to quantitate retinal thickness and volume and perform analysis of retinal topography. Currently, commercial SD-OCT instruments are used routinely in clinical practice to obtain morphologic information used to diagnose and manage patients with various retinal disorders including macular degeneration and diabetic retinopathy. Newer swept-source OCT technology with faster image acquisition, provides wider field imaging of the peripheral retina. SD-OCT instruments can be incorporated into surgical microscopes to allow imaging of the retina during retinal surgery so that morphologic changes in the retina from surgical maneuvers can be observed in real time. More recently, OCT angiography (OCTA) has been developed which allows rapid, non-invasive 3D imaging of retinal and choroidal vascular flow. This is achieved by processing rapid serial SD-OCT images to detect movement of blood cells within vessels. Research has been done to further improve image resolution of SD-OCT to a cellular level by adding adaptive optics (AO) technology. The latest in SD-OCT technology is optoretinography (ORG), a technique to derive functional information from OCT images of the retina.

**Conclusions:** Advancement in OCT technology has made it possible to obtain high resolution retinal images that can provide anatomic, physiologic and functional information of the retina in live patients.

**Keywords:** Optical coherence tomography (OCT); optical coherence tomography angiography (OCTA); optoretinography (ORG); retina

Submitted Nov 28, 2024. Accepted for publication Mar 24, 2025. Published online Apr 29, 2025.

doi: 10.21037/atm-24-211

**View this article at:** <https://dx.doi.org/10.21037/atm-24-211>

<sup>^</sup> ORCID: 0000-0001-5911-6671.

## Introduction

The retina is a highly specialized neural tissue that lines the back of the eye. It is the primary neurosensory tissue in the eye that initiates visual signal processing, making vision possible. The retina is organized into distinct cellular layers which can be visualized *in vivo* using an imaging technology called optical coherence tomography (OCT) (*Figure 1*). OCT can provide near histologic image resolution of the retinal layers quickly and non-invasively. As such, OCT has become an invaluable tool in diagnosis and management of retinal disorders that affect vision. In this narrative review, we will discuss the anatomy of the retina and the associated vascular supply as background for the clinical applications of OCT. An overview of the development of OCT over the last three decades will be discussed to highlight the latest advancements in this imaging technology that have resulted in improved clinical application of this technology.

### *Background: anatomy of the retina*

The retina is an intricately organized tissue with distinct cellular layers (*Figure 1*). The outermost layer of the retina is the retinal pigment epithelium (RPE), a monolayer of pigmented cells situated between the neural retina and the choroid. The choroid provides vascular supply to the RPE and photoreceptors, the main neuronal cells in the outer retina (1). The RPE serves many essential functions, including absorption of excess light, transport of nutrients, phagocytosis of photoreceptor outer segments, and maintenance of retinal homeostasis, in particular recycling photopigment and breaking down waste products from the absorbed photoreceptor outer segment material (2).

Above the RPE lies the neurosensory retina, which consists of multiple layers of specialized neuronal cells responsible for processing visual information. The layers of the retina are oriented in such a way that the photoreceptor cells are closest to the RPE, with subsequent layers stacked internally in the eye toward the vitreous cavity (3). The photoreceptor layer in the outer retina contains the somata and the inner and outer segments of rods and cones, responsible for capturing light (4). Just within the photoreceptor layer is the external limiting membrane (ELM) which serves as a barrier-like structure that separates the inner segments of photoreceptor cells (housing mitochondria) from the outer nuclear layer (ONL) where the retinal Muller glial cells join the photoreceptor cells (5). It functions to maintain the integrity and organization

of the photoreceptor layer (6). The ONL, containing the cell bodies of photoreceptors, is just above the outer plexiform layer (OPL), where photoreceptors synapse with bipolar and horizontal cells (7,8). Some very early processing steps of the visual signal happen at this junction, such as rapid motion detection and contrast enhancement. The inner nuclear layer (INL) contains the cell bodies of bipolar, horizontal, and amacrine cells, which mediate synaptic connections between photoreceptors and ganglion cells. The inner plexiform layer (IPL) houses synaptic connections between bipolar, amacrine, and ganglion cells, allowing for the integration and refinement of visual information (9). Finally, the ganglion cell layer (GCL) holds the somata of ganglion cells. The axons of these ganglion cells collectively form the retinal nerve fiber layer (RNFL) before converging at the optic disc and forming the optic nerve (10). On the inner border of the RNFL is the inner limiting membrane (ILM), a thin, acellular layer that forms the interface between the retina and the vitreous humor; ILM provides structural support and anchoring for the retinal tissue (11). *Figure 1* is a cross-sectional OCT image showing the various retinal layers. The integrity of these retinal layers is clinically relevant, as many conditions selectively affect one or more specific layers within the retina. The ability to distinguish and monitor these layers in the retina on OCT images can provide critical information for diagnosing and managing retinal disorders.

The retina can be further categorized into two distinct regions: the central retina and the peripheral retina (12). Situated at the posterior pole of the eye, the central retina encapsulates the macula, a specialized area responsible for central vision, which in turn contains the fovea centralis, a small depression in the center of the macula (*Figure 1*). In the fovea, cone photoreceptors are densely packed to provide high acuity and color central vision. Clear central vision allows tasks like reading and recognizing faces to be performed (13-15). Cone photoreceptors in the fovea have a one-to-one synaptic connection with bipolar cells. The dense photoreceptor packing in the fovea translates to high acuity vision. The cones and rods are at about equal density between 400–500  $\mu\text{m}$  from the fovea, i.e., periphery of macula, after which the retina becomes rod dominant. The rod dominant peripheral retina provides night and peripheral vision and motion detection (13-17). The peripheral retina extends from the outer edge of the macula to the ora serrata, the transition zone where the retina ends. In the peripheral retina, there is greater convergence of photoreceptors to bipolar cells and further convergence

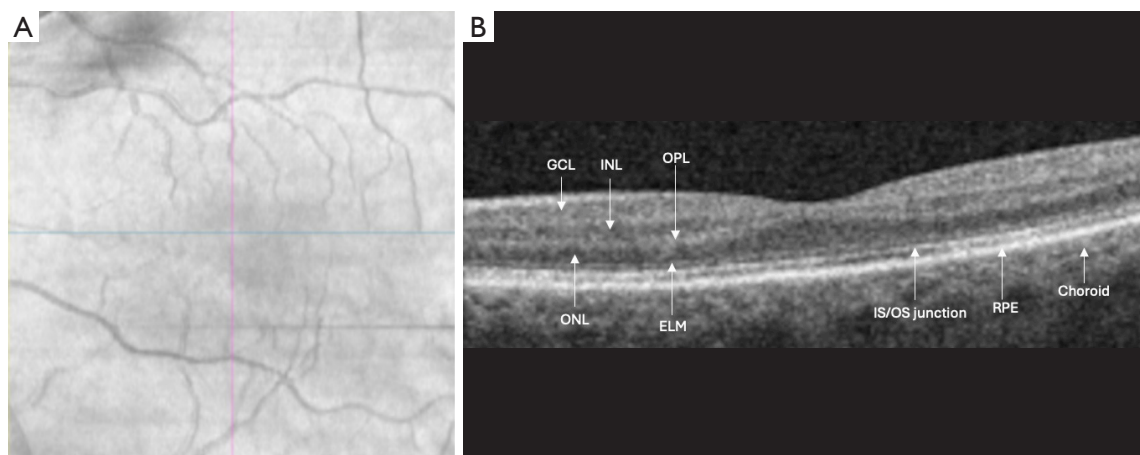


**Figure 1** OCT image of the central retina, i.e., macula, showing the various layers of the retina. (A) *En face* near-infrared reflectance image of the macula. The blue horizontal line in (A) indicates the location of the OCT scan in (B). The red vertical line in (A) indicates the location of the vertical OCT scan of the macula that was simultaneously generated by the OCT machine but not included in this figure. (B) Cross-sectional B scan OCT image of the macula including the fovea (central depression) with the various retinal layers identified. ELM, external limiting membrane; GCL, ganglion cell layer; INL, inner nuclear layer; IS/OS junction, inner segment/outer segment junction of the photoreceptor layer (also called ellipsoid zone); OCT, optical coherence tomography; ONL, outer nuclear layer; OPL, outer plexiform layer; RPE, retinal pigment epithelium.

of bipolar cells to the ganglion cells. The result is the peripheral retina having a decrease in acuity but greater aggregate and spatial processing for motion detection (4,13).

The blood supply of the retina comes from two primary sources: the central retinal artery and the choroid (18). The central retinal artery, a branch of the ophthalmic artery, enters the eye through the optic nerve and branches extensively to provide blood supply to the inner layers of the entire retina (19). Complementing this vascular supply is the choroid, a highly vascular layer located directly beneath the RPE (Figure 1). The choroid contains the choriocapillaris, a dense network of blood vessels that provides the blood supply to the outer layers of the retina, including the photoreceptors and RPE (20). This dual blood supply to the retina ensures efficient oxygenation and nutrient delivery to the entire thickness of the retina. This vascular arrangement addresses the significant metabolic demands of the retina. The unique structure of the fovea, which is devoid of the inner retinal layers and supplied purely by the choroid, allows light to reach the photoreceptor cells directly and without obscuration from the presence of any overlying inner retinal neurons.

### **Rationale and knowledge gap**

Given its complex anatomy, it is difficult to evaluate the

morphologic changes in the retina in live patients purely based on clinical examination. A non-invasive imaging method to rapidly evaluate the various layers of the retina in live patients is invaluable in diagnosis and management of patients with various retinal disorders. This is possible using OCT imaging of the retina. In this narrative review, we provide an overview of the technological advancements in OCT imaging that allow rapid *in vivo* imaging of the retina in live patients to obtain morphologic, vascular flow and even functional information that can be used in our clinical management of patients with retinal disorders. We present this article in accordance with the Narrative Review reporting checklist (available at <https://atm.amegroups.com/article/view/10.21037/atm-24-211/rc>).

### **Methods**

This narrative review summarizes the technical development and clinical applications of OCT retinal imaging. This review was written based on literature searches conducted by authors using the PubMed database between September 2023 to April 2024 (Table 1). It also includes information obtained from authoritative texts and information provided by the authors based on their research on OCT imaging and their expertise as experienced ophthalmologists treating patients with retinal disorders.

**Table 1** The search strategy summary

Items	Specification
Date of search	Sep 01, 2023 to Apr 30, 2024
Database	PubMed
Search terms used	Optical coherence tomography retina; spectral-domain OCT of retina; Fourier-domain OCT of retina; swept source OCT; optical coherence tomography angiography; phase variance OCT; retinal anatomy; adaptive optics-OCT; intraoperative OCT; optoretinography
Timeframe	No limit
Inclusion criterion	English only
Selection process	All authors conducted the selection and consensus was obtained via discussion among all authors

OCT, optical coherence tomography.

### **OCT: *in vivo* cross-sectional imaging of the macula**

OCT has revolutionized the diagnosis and management of retinal pathology, especially macular pathology. OCT can generate high-resolution, cross-sectional images of the retina quickly in live patients. Its ability to image the various retinal layers and localize associated pathologic processes makes OCT an indispensable tool in the current clinical practice of ophthalmology.

The underlying principle of OCT imaging is interferometry, a technique used to measure and analyze interference patterns generated by two or more coherent light waves (21). OCT utilizes low-coherence interferometry that begins with a broad-spectrum light source. The light is then split into two arms: a sample arm and a reference arm. In the sample arm, light is directed into the eye to scan various tissues. As light interacts with tissue, it is reflected back towards the OCT machine; each light reflection is affected by the tissue's intrinsic properties and the depth of the object scattering the light (21,22). Meanwhile, the light in the reference arm is directed towards a mirror, which then reflects it back toward the detector. These two returning light waves, having traveled different distances, are slightly out of phase. When they arrive together at the detector, they produce an interference pattern, known as an interferogram, which can be analyzed to unveil depth-coded information and generate an image (21). While OCT technology can provide images of different parts of the eye, including the anterior segment and optic nerve head, this review will focus on OCT imaging of the retina and choroid to diagnose and manage retinal disorders.

The OCT image is generated from a series of “A-scans” that are combined to form a two-dimensional (2D), cross-

sectional “B-scan” image. The “A” and “B” scan terminology used in OCT imaging is adapted from ultrasonography. The A-scan is generated when light passes into the eye at a single point and is reflected back by the various layers of the retina. This provides information about the internal structure of the tissue at that specific point, with intensity proportional to the reflectivity of a given tissue (23). By adding a scanning mirror to move the incident light laterally, multiple A-scans can be acquired to generate cross-sectional images, or B-scans, of the tissue. The B-scan OCT image of the retina is a 2D cross-sectional image of the retina providing reflectivity information of the various retinal layers (*Figure 1B*) (24). The B-scan OCT image is commonly used to access the integrity and morphology of the various retinal layers and assess retinal thickness. Although OCT can be used to image different parts of the retina, it is most commonly used to image the macula and diagnose maculopathy. It is commonly used to diagnose and monitor macular changes associated with various retinal diseases, such as macular edema (25), macular holes, macular degeneration and retinal detachment. Volumetric or three-dimensional (3D) images of the retina (macula), are produced by stacking adjacent 2D B-scan images (26). This 3D reconstructed OCT image can be used to visualize structures within the retina from various angles and depths. The 3D volumetric images of the retina can be used to generate *en face*, i.e., C-scan images, of the various layers of the retina. Similarly, OCT can also be used to image the optic nerve head to evaluate optic neuropathy and glaucoma and associated changes in the RNFL thickness. These OCT changes can be obtained serially to evaluate for progression of these conditions.

OCT enables clinicians to visualize and quantify

**Table 2** OCT changes associated with common retinal disorders involving the macula

Retinal disorder	Subretinal fluid on macular OCT	Intraretinal fluid on macular OCT	Other characteristic OCT findings
AMD, non-advanced	No	No	Drusen, PED
AMD, neovascular or exudative	Yes	Yes	Drusen, PED, SHRM
AMD, advanced with geographic atrophy	No	No	Drusen, PED, focal loss of outer retinal layers with hyperreflective shadowing into choroid
Diabetic retinopathy with macular edema	Only in severe cases	Yes	Intraretinal hyper-reflective foci may be present from exudates
Central serous retinopathy	Yes	No	Small PED; pachychoroid*
Epiretinal membrane/ macular pucker	Rarely in severe cases	Yes in more severe cases	Hyperreflective linear structure on the retinal surface; retinal surface irregularity; loss of foveal depression
Retinal detachment	Yes if macula involved	No	SRF may vary with head position if serous retinal detachment
Uveitic macular edema	Some forms of uveitis	Yes	Possible hyperreflective foci in the vitreous cavity from vitreous cells

\*, the choroidal layer on OCT will be thicker than the overlying retinal layer in eyes that are pachychoroid. AMD, age-related macular degeneration; OCT, optical coherence tomography; PED, pigment epithelial detachment (i.e., focal elevation of the retinal pigment epithelium); SHRM, subretinal hyperreflective material; SRF, subretinal fluid.

structural changes within the retina, allowing for early detection and precise monitoring of disease progression. Importantly, OCT can reveal pathological changes that may not be apparent on clinical examination alone. For example, subtle signs of macular edema or subretinal fluid accumulation, indicative of various retinal disorders, may be missed during routine eye examination but readily identified on OCT scans (*Table 2*) (25). By providing detailed, quantitative information about retinal morphology and pathology, OCT enhances diagnostic accuracy, guides treatment decisions, and enables timely intervention to preserve vision and prevent irreversible damage to the retina. The non-invasive nature and ability to perform rapid, repeatable scans make OCT an indispensable tool in the comprehensive evaluation of retinal diseases.

### ***OCT: advancement in image acquisition speed and resolution***

The first-generation OCT instrument developed for cross-sectional imaging of the retina *in vivo* used time-domain OCT (TD-OCT) which uses a physically moving mirror to obtain a signal (21,27,28). Using TD-OCT, image acquisition speed is limited by the movement of the mirror such that only a limited number of A-scans of the retina can be obtained without eye movement artifacts. The result is an OCT cross-sectional B-scan image with limited image

resolution (*Figure 2A*) (21,27-29). The only commercial TD-OCT instrument was the Stratus OCT (Zeiss Meditec, Oberkochen, Germany). Using the Stratus TD-OCT, only six radial B-scans of the macula could be obtained, limiting our ability to evaluate the entire macula.

Subsequent introduction of spectral-domain OCT instruments [SD-OCT, also called frequency or Fourier domain-OCT (FD-OCT)] refined the signal of obtained retinal images and expanded the capabilities of the instrumentation (*Figure 1* and *Figure 2B*) (23,28,30). Instead of a physically moving mirror used in a TD-OCT instrument, SD-OCT utilizes a spectrometer to detect the frequency of reflected light, which is then transformed back for spatial information. The transition to SD-OCT from TD-OCT resulted in significantly faster image acquisition. By increasing the rate at which A-scans can be obtained, a higher density of A-scans can be used to generate a B-scan OCT image without increasing the amount of time to acquire the images. With SD-OCT, scan speed is increased to 50,000 A-scans/s or more (31,32), resulting in improved lateral image resolution (the resolution in the axial plane is dependent on the light source). Faster imaging reduces the incidence of motion artifact and allows for acquisition of a greater number of B-scan images in a relatively short time. In turn, higher density serial B-scans can be obtained and used to create 3D-volumetric images of the macula. The result is a more complete imaging of the entire macula



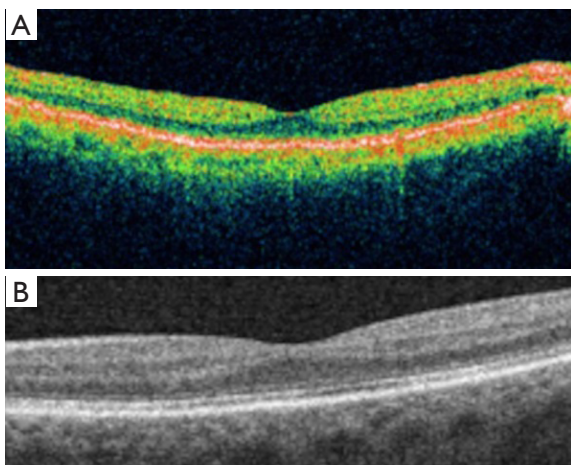


**Figure 2** Time domain versus SD-OCT image of a normal macula. (A) TD-OCT image is displayed in pseudo-color to highlight the various layers of the retina (green) from the RPE (red). Note that the retinal layers are not clearly visualized. (B) SD-OCT image showing the various layers of the retina that can be visualized clearly even using grayscale. TD-OCT image has lower image resolution due to lower sampling when compared to the faster SD-OCT image. Improvements in light sources also improved the axial resolution of SD-OCT image when compared to TD-OCT such that the retinal layers are more clearly visualized. RPE, retinal pigment epithelium; SD-OCT, spectral domain optical coherence tomography; TD-OCT, time domain optical coherence tomography.

with increased sensitivity to detect abnormalities within the retinal layers (*Figure 1*) (33).

Around the time that SD-OCT instruments were being developed, advances in light sources provided additional improvement in OCT image resolution (32,34,35). The axial resolution of OCT images is based on the breadth of frequency of the light used to obtain the image. Broadband light sources allow for greatly improved axial resolution of OCT images (36,37). TD-OCT systems using older light sources had axial resolutions of around 10  $\mu\text{m}$ , whereas current SD-OCT instruments can achieve axial resolutions of up to 2  $\mu\text{m}$  (32,34). The improved axial image resolution allows improved resolution of the various layers of the retina. While the advancement in light source could improve the axial resolution of TD-OCT as well, SD-OCT, with faster image acquisition time, was able to optimize both the axial and transverse image resolution of the OCT image.

Further advances in light source technology allowed for even faster image acquisition times with the development of

swept source OCT (SS-OCT), a type of SD-OCT (38,39). In SS-OCT, the light source “sweeps” through a range of wavelengths rather than a broadband source of light (38,39). This provides a couple of advantages. One is that the range of wavelengths used extends further than that of a single source. Using the longer wavelength end of the spectrum of the light source allows for deeper penetration into tissue and imaging of structures that may be obscured using standard FD-OCT. An example is imaging of the choroid which can be imaged more completely using SS-OCT as there is less overall reflection from the overlying retinal tissue (40). Similarly, SS-OCT allows imaging of deeper optic nerve structures, such as the lamina cribrosa (41). SS-OCT also allows for improved image acquisition speed since the light source “sweeps” through a range of wavelengths very quickly and faster cameras are available to sample the signals (39) at various wavelengths. As a result, some SS-OCT instruments can offer wide field OCT imaging capabilities such that the macula and peripheral retina can be imaged simultaneously (42). SS-OCT is becoming more prevalent in retinal imaging, but the use of commercial SS-OCT instruments in clinical practice has been less popular than expected, possibly due to increased cost.

### *Clinical applications of OCT retinal imaging*

Improved transverse and axial resolution made possible using SD-OCT instruments allows *in vivo* analysis of retinal morphology with image resolution approaching that of traditional histology (*Figure 1*). Each of the bright and dark bands seen in the SD-OCT B-scan of the macula have been correlated with the histologic layers of the retina (43–45), though some debate remains regarding the subcellular nature of some of these features. For example, one of the outer retinal bands on OCT B-scan is believed to represent either the junction of the photoreceptor inner and outer segments or the ellipsoid of the inner segment (35,45,46). SD-OCT imaging has improved our understanding of the pathogenesis of various retinal conditions and provided biomarkers to access prognosis and treatment outcome of these various retinal conditions. For example, subtle disruptions in the photoreceptor layer on SD-OCT has been identified in eyes with previously unexplained vision loss (47). Furthermore, choroidal neovascularization associated with exudative age-related macular degeneration (AMD), traditionally diagnosed using fluorescein angiography, can be visualized using SD-OCT 3D imaging and localized to subretinal or sub-RPE



**Figure 3** The map of the nine zones of the macula based on the ETDRS macula grid is denoted in green and overlaid on a fundus image of the macula. Note that each of the nine zone has a numerical value which corresponds to the retinal thickness of the macula in that sector of the macula in micrometers. Each of the nine zones is denoted in green color in this map, indicating that the macular thickness is within the normal range for all zones. Macular thickness that falls outside the normal limits are represented by color other than green to denote abnormality. ETDRS, early treatment of diabetic retinopathy study.

space (48). This additional anatomic information allows us to further characterize choroidal neovascularization with different prognoses.

Currently available commercial SD-OCT instruments have built-in segmentation algorithms that create detailed thickness maps of the macula. As shown in *Figure 3*, the macular thickness map of a commercial SD-OCT instrument divides the macula into 9 zones, based on regions used in the Early Treatment for Diabetic Retinopathy Study (ETDRS). The thickness measurement of each of these 9 zones are provided numerically and denoted by different colors, depending on whether the thickness is increased, normal or decreased. The OCT macular thickness measurements and qualitative assessment of the individual high-resolution B-scan OCT images of the macula are used routinely to monitor for changes in the macula associated with various retinal diseases. Repeatability of OCT macular and RNFL thickness measurement using commercial SD-OCT is high using the same instrument and eye tracking but can vary somewhat among different commercial OCT instruments due to differences in segmentation algorithm (49,50). The OCT macular thickness measurement has been used to monitor treatment effect in clinical trials as well as clinical practice (51-53). Macular thickness measurement

and presence or absence of intraretinal and subretinal fluid on OCT B-scans have become biomarkers used as an endpoint for treatment of choroidal neovascularization and macular edema associated with common retinal disorders such as AMD and diabetic retinopathy (*Figure 4*) (54,55). *Table 2* provides a summary of common retinal conditions associated macular changes on OCT.

While early clinical TD-OCT instruments provided some cross-sectional information of the macula used to diagnose maculopathy such as macular holes, epiretinal membranes (ERMs), and intra- or subretinal fluid (29), the higher density B-scans with higher axial resolution, decreased signal-noise ratios possible using SD-OCT have allowed diagnosis of more subtle changes in the macula. Small abnormalities limited to specific retinal layers, not visualized using earlier generation TD-OCT instruments, can be well visualized using the current SD-OCT technology, improving our diagnostic ability (33,47).

Improved diagnosis and characterization of specific macular disease states became possible as image quality improved using SD-OCT (*Table 2*). SD-OCT allowed improved diagnosis of ERM involving the macula when compared to TD-OCT and clinical exam (56). In addition, SD-OCT allowed visualization of associated morphologic changes in the macular layers that correlates with decrease in visual acuity in eyes with ERMs (56). In eyes with non-exudative AMD, characteristic SD-OCT findings have been identified as risk factors for progression to exudative AMD. They include, low lying wide pigment epithelial detachment (PED), also called “double layer sign”, subretinal hyperreflective material (SHRM) and intraretinal hyperreflective foci (*Figure 4*). By monitoring for the presence of these OCT findings, risk of progression to exudative AMD can be better estimated by clinicians. In eyes with non-exudative AMD, areas of incomplete and complete RPE and outer retinal atrophy on OCT imaging are of interest and demonstrate a potential nidus of geographic atrophy, a sign of advanced nonexudative AMD (*Figure 4B*) (57). These OCT features have been used to identify patients at risk for vision loss from atrophic advanced non-exudative (“dry”) AMD.

With the development of SS-OCT for wide-field imaging there is an increased ability to image lesion in the peripheral retina. Using wide-field OCT, peripheral retinal elevation from a retinal schisis (a separation of layers within the retina) can be differentiated from a retinal detachment (where the retina is separated from the underlying RPE), a distinction which can be challenging on clinical exam. Wide-field OCT imaging also allows the entirety of large

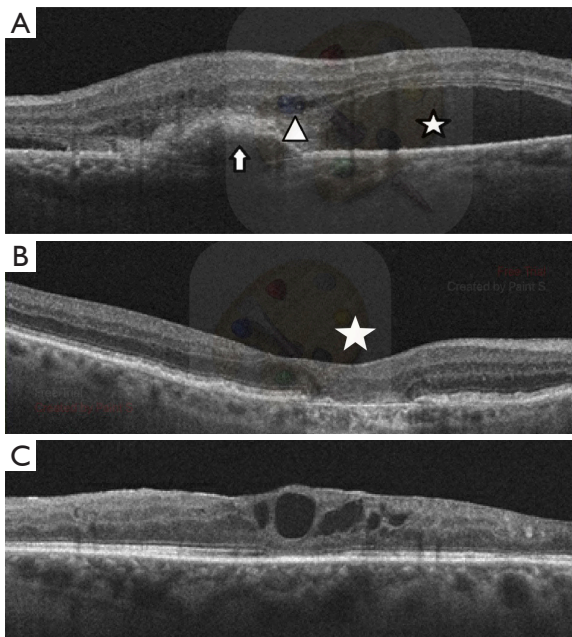


**Figure 4** SD-OCT cross-sectional image of the macula of eyes with common macular disorders. (A) An eye with exudative age-related macular degeneration. The arrow indicates the RPE which becomes elevated due to choroidal neovascularization. Intraretinal fluid (arrowhead) and subretinal fluid (star) are signs of active exudative age-related macular degeneration in this OCT image. OCT images are repeated over time to monitor disease response to treatment, i.e., intravitreal injection of drugs that inhibit vascular endothelial growth factor, based on resolution of subretinal and intraretinal fluid. (B) An eye with geographic atrophy from advanced nonexudative or “dry” age-related macular degeneration showing focal loss of RPE and photoreceptor layer (star) just nasal to the fovea. There is increased light transmission in the region of RPE loss as manifested by increased reflectance of the OCT signal in the underlining choroidal layers. (C) An eye with diffuse macular edema from diabetic retinopathy. Note that the inner retinal layers are thickened and somewhat blurred with cystic spaces within the inner retinal layers from intercellular and intracellular fluid accumulation within the retinal layers. OCT, optical coherence tomography; RPE, retinal pigmented epithelium; SD-OCT, spectral domain optical coherence tomography.

peripheral lesions to be captured in a single image.

### Going deeper—enhanced depth imaging

While most of the attention using OCT imaging has been on the retina, many conditions affect the choroid

which is less well visualized using OCT. Multiple physical limitations play a role in limiting OCT visualization of the choroid including wavelength of the light source as well as the way that light is focused on the tissue and then detected. The default setting is optimized for clarity within the retinal layers (41,58). Wavelength of light also plays a role—longer wavelength light can penetrate deeper tissues due to a decrease in light scattering. By adjusting OCT imaging parameters, improved resolution of deeper structures can be obtained using SD-OCT. An example of this is enhanced depth imaging OCT (EDI-OCT). This adjustment available in commercial SD-OCT instruments changes the “focus” of the camera to deeper structures in the eye and allows for improved image resolution of the choroidal layer. As noted above, SS-OCT can also improve penetration to these deeper layers by sweeping through longer wavelengths. Conditions that primarily affect the choroid have been identified as a result. An example is the so-called “pachychoroid spectrum” of conditions, such as polypoidal choroidal vasculopathy and central serous chorioretinopathy, which is characterized by a thickened choroidal layer in the macula on EDI-OCT images (59). Tumors of the RPE and choroid can also be better characterized and imaged using EDI-OCT. Characteristics of specific posterior segment eye tumors such as the tumor depth and extent of involvement, presence of associated subretinal fluid and contour of the tumor can be obtained using EDI-OCT imaging which aids in diagnosis (*Figure 5*). Treatment response may also be tracked using EDI-OCT by making comparative measurements of lesion size and associated morphologic changes in the retina over time. Finally, with recent advances in suprachoroidal drug delivery, OCT with deeper penetration can be used to help confirm drug delivery in this space.

### OCT angiography (OCTA)

Angiography, using fluorescein or indocyanine green (ICG) dye, has long been the standard imaging method to evaluate the retinal and choroidal vasculature and flow. However, these invasive procedures require an intravenous injection of contrast dye, are time-consuming and provide only 2D image information.

Retinal and choroidal flow can be imaged *in vivo* in 3D by using standard SD-OCT instruments with software modifications. By rapidly obtaining multiple SD-OCT images of the same region of the retina and determining dynamic portions of the image, a motion contrast image



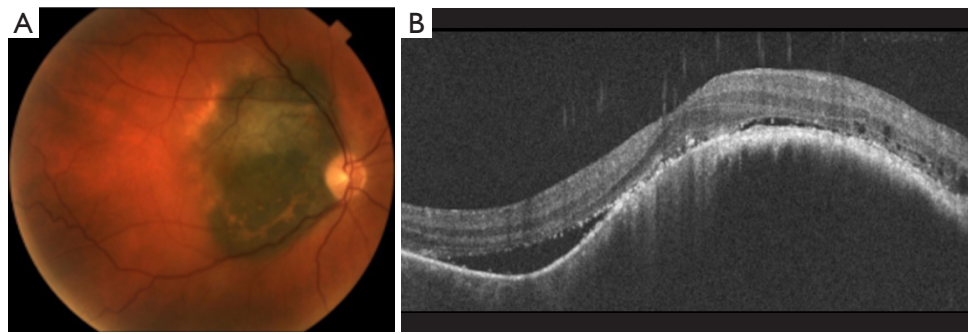


**Figure 5** Images of an eye with choroidal melanoma involving the macula. (A) Color fundus photograph of the right eye of a patient with choroidal melanoma adjacent to the optic nerve and involving the nasal macula. (B) Enhanced depth imaging SD-OCT cross-sectional image of the macula and through the choroidal melanoma showing the presence of subretinal fluid over the elevated choroidal tumor, a sign of exudation from tumor growth. SD-OCT, spectral domain optical coherence tomography.

is formed which detects movement of blood cells within vessels. The resulting angiographic image from serial OCT scans is termed OCTA (60). Other terms used for OCTA in earlier studies include phase-variance or phase-contrast OCT or power-doppler OCT, depending on the software used to generate OCTA images (61,62). The advantages of OCTA imaging over traditional fluorescein angiography include rapid image acquisition without using intravenous contrast. However, fluorescein angiography cannot be completely replaced by OCTA since retinal vascular filling time and vascular leakage cannot be determined using OCTA (61). These are important angiographic findings that may be critical in diagnosing certain retinal vasculopathies.

One distinct advantage of OCTA over contrast-based angiography is the three-dimensionality of the images. Not only can the location of perfused vessels be mapped, but the depth of the affected vascular networks can be determined by choosing specific strata within the cross-sectional OCTA images. The 3 separate retinal capillary plexus layers—superficial, middle and deep—can be separately imaged using OCTA by selecting the depth within the retina to be analyzed. Most commercial OCTA software is preset to segment OCTA images into two plexus layers, superficial and deep. Some commercial OCTA systems also provide automated quantification of vascular density for the retinal layers (63–65). The automated quantification of the vascular density is repeatable but can be affected by morphologic changes such as macular edema (66,67). Foveal avascular zone area can also be measured using commercial OCTA instruments with high repeatability (63,68).

The depth information of retinal vascular flow provided by OCTA, not available with a 2D fluorescein

angiogram, can be invaluable clinical information for diagnosis of certain clinical entities. Conditions such as paracentral acute middle maculopathy and acute macular neuroretinopathy, can only be diagnosed using OCT and OCTA since retinal vascular non-perfusion is localized within the deeper retinal vascular plexus layers of the macula (69). In eyes with macular telangiectasia, subtle retinal vascular changes in the macula have been noted even in the earliest stages of this condition which is thought to be associated with Muller cell degeneration (62). Furthermore, the 3D retinal vascular flow information obtained using OCTA has improved our understanding of pathogenesis of vision loss associated with common retinal vasculopathies, such as diabetic retinopathy (70,71).

The vessel depth also can be used to diagnose abnormal retinal or choroidal neovascularization which requires prompt intervention to minimize risk of vision loss. Retinal neovascularization is seen on the surface of the retina in eyes with severe retinal ischemia, such as proliferative diabetic retinopathy. The surface location of this abnormal vascular proliferation can be imaged using OCTA to differentiate it from intraretinal vascular anomalies (72). Similarly, choroidal neovascularization, characterized by abnormal subretinal or sub-RPE fibrovascular proliferation, can be visualized using OCTA (61,73). Prompt diagnosis of choroidal neovascularization is important so that intervention can be initiated to minimize severe vision loss. The presence of intra and subretinal fluid on OCT and/or hemorrhage on funduscopy can provide clinical evidence of exudation which is used to confirm the diagnosis of active choroidal neovascularization that warrant treatment (*Figure 4A*). By segmenting the deep outer retinal layers and the subretinal/

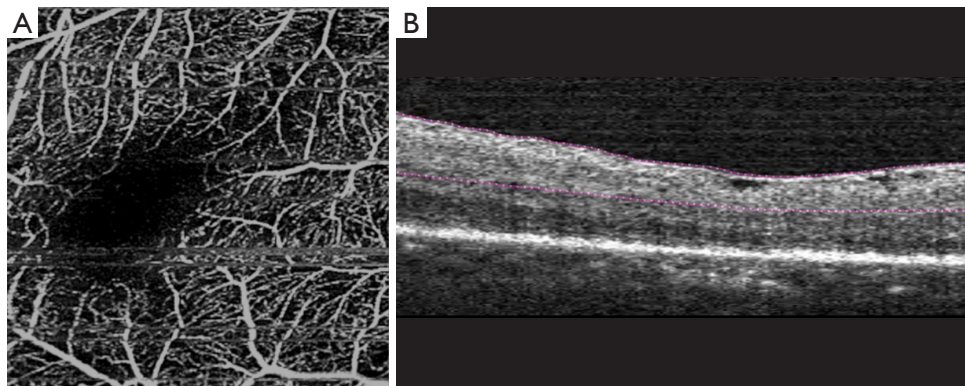


**Figure 6** OCTA with motion artifacts. (A) The *en face* OCTA image shows the branching pattern of vascular flow detected within the retinal circulation. Some horizontal lines are present in the image that correspond to motion artifacts resulting from eye movement during image acquisition. Note the discontinuity in the retinal vascular flow pattern on either side of these artifacts. Such movement artifacts can prevent accurate quantification of vascular flow. (B) Corresponding spectral domain OCT B-scan of the same eye just superior to the fovea is shown. The dashed colored lines within the B-scan OCT image represent the segmentation of the retina that corresponds to the area imaged in OCTA image (A). OCT, optical coherence tomography; OCTA, optical coherence tomography angiography.

sub-RPE layers in the OCTA image, subretinal or sub-RPE neovascularization may be detected as these deeper outer retinal layers which are normally avascular. Some commercial OCTA systems have preset settings that allow automated segmentation of these layers to aid in diagnosis.

OCTA imaging also allows visualization of flow changes in the choroid. In eyes with atrophic AMD, flow voids in the choriocapillaris near geographic atrophy can be clearly visualized (74). In eyes with posterior uveitis, such as acute posterior multifocal placoid pigment epitheliopathy (aka APMPE), focal flow deficits in the choriocapillaris may be visualized using OCTA which normalizes with resolution of the condition (75).

A limitation of using OCTA in clinical practice is the presence of image artifacts. Clinicians should be aware that artifacts can be present in the OCTA image that can give the false impression of blood flow in areas where there is none. One artifact that is common to any form of ophthalmic imaging is motion artifact. Given the *en face* nature of OCTA images, motion artifact may appear as a distortion of vessels or may cause a gap in the retinal area covered, making accurate interpretation difficult or impossible at times (Figure 6). An artifactual finding more specific to OCTA is projection artifact—this occurs when light passes through moving blood and is reflected back by the RPE (76,77). Projection artifact can result in blood flow being detected in the RPE or outer retina that mirrors vascular flow detected in the inner retina (77,78). Since the RPE and outer retina are normally devoid of blood flow,

projection artifacts can be confused for anomalous vessels along the RPE such as choroidal neovascularization (76). Conversely, highly reflective structures can reduce or even eliminate the OCTA signal below them, appearing as a loss of perfusion where there may be normal flow (78). Finally, OCTA signals at various layers of the retina depend on correct segmentation of the layers on the OCTA image; errors in OCT segmentation in eyes with retinal morphologic changes can erroneously change the vascular flow information obtained in different retinal layers. Various studies have shown that repeatability of retinal vascular density measurements using commercial OCTA instruments is high but some reduction in OCTA vascular density repeatability was observed eyes with retinal morphologic changes, such as macular edema (66,79).

### *OCT in the operating room*

Having high-resolution cross-sectional imaging of the retina using SD-OCT in the clinic provides numerous benefits as outlined above. Now, SD-OCT imaging also can be obtained intraoperatively using OCT instrumentation that is incorporated into the surgical microscope. The structural information of the retina obtained using SD-OCT can be invaluable in surgical management of various retinal conditions. One such area is surgery for removal of ERM where the use of intraoperative OCT (iOCT) can improve surgical success and outcome by improving our ability to visualize the ERM (56). iOCT also may be used to

assist in identifying ideal locations to initiate ERM removal during surgery; iOCT can be used just after ERM removal to ensure complete removal of the ERM. It has been shown that iOCT changes in macular morphology just after ERM removal can be predictive of long-term anatomic outcome after surgery (80). Similarly, iOCT has been shown to provide information that may be important for other macular surgeries, including macular hole surgery where it can confirm peeling of the ILM (81). In cases of surgery for vitreomacular traction syndrome, iOCT has been used to confirm intraoperatively that the surgery performed was adequate to completely relieve macular traction (82).

### ***Research grade instrumentation: what the future may hold***

Clinical-grade commercial SD-OCT instruments offer high resolution images, but image resolution is limited to about 5  $\mu\text{m}$  axially and about 15  $\mu\text{m}$  transversely (31,32). Incorporating adaptive optics (AO) into OCT instrumentation (AO-OCT) significantly increases transverse resolution of the OCT image to around 3  $\mu\text{m}$ . Currently, AO-OCT is available only for research; it is a valuable tool as it allows for visualization of individual cells in the retina. By obtaining images of finer structures in the retina, and increasing the resolution of the image, further information of cellular changes in the retina can be obtained *in vivo*. For example, AO-OCT has been used to visualize intraretinal cellular changes in an eye with hereditary maculopathy treated with intravitreal injection of autologous CD34<sup>+</sup> stem cells in a clinical trial (83). Using AO-OCT, researchers have provided additional evidence for the origin of retinal bands seen on standard OCT images (Figure 1). For example, AO-OCT imaging was used to show that the inner-segment outer-segment junction of photoreceptor is a source for the hyperreflective outer retinal band after the ELM, rather than “ellipsoid zone”. Additionally, AO-OCT has been used to image individual ganglion cells in healthy and diseased retinas, such that more accurate and detailed assessment of ganglion cell loss can be obtained than measuring gross thickness of the RNFL or GCLs using SD-OCT (84,85). While the processing steps required to obtain AO-OCT images is cumbersome and labor intensive, these research-grade instruments allow us to gain new insights into pathogenesis of retinal diseases and improves our understanding of observations made using clinical-grade OCT instruments.

An emerging avenue of investigation in retinal imaging is the development of functional assays using imaging

technology. Optoretinography (ORG) is a term that encompasses a number of different techniques to make functional measurements in retinal tissue exposed to a light stimulus. The signal being measured in ORG techniques includes changes in cellular reflectivity in *en face* retinal imaging modalities (such as scanning light ophthalmoscopes), or a shift in the way light is scattered as measured using SD-OCT (86). These ORG measurements can be made with high-resolution AO-OCT instruments, but recent reports also demonstrate that a response is measurable using clinical-grade SD-OCT instrumentation (87). Other forms of ORG measurements have been made in various diseased retinas, but there remains much work that needs to be done to develop this novel technology for clinical applications. There is a potential possibility that imaging-based functional assays, such as ORG, may become available in the clinic such that OCT could potentially be used in clinical ophthalmologic practice to obtain structural and functional information simultaneously.

### ***Strengths and limitations***

This article provides a comprehensive review of OCT development for retinal imaging and corresponding clinical applications. The strength of the article is that it is written for a broad range of readers, including readers with minimal background in ophthalmology as well as current eye researchers. Additional strength of this article is that the lead authors are clinicians with expertise in treating retinal disorders who use OCT imaging regularly in their clinical practice. Furthermore, the lead authors have conducted extensive prior research in retinal imaging, including OCT imaging. As such, some of the clinical applications discussed in this article are based on common clinical practice or prior research conducted by the authors. Although this article is not a systemic review of the topic, literature search was conducted by the authors and the most relevant published papers that may be of interest to the readers were selected for inclusion in this review. The limitation of this study is that not all published articles on the topic are included given the word limitation of this article. In addition, we limited this article to OCT imaging of the retina and choroid. However, OCT also can be used to image other ocular structures including the cornea and optic nerve. Changes in RNFL thickness on OCT have been used to monitor glaucoma, and deep learning models are being developed for this purpose (88). Retinal OCT and OCTA changes are being explored as biomarkers for neurologic

diseases, such as Alzheimer's and Parkinson's disease (89-91). It is beyond the scope of this article to cover these other applications. Topics that may be of particular importance or interest to certain readers may not be discussed in detail in this review article. Thus, the authors encourage such readers to conduct their own literature search on the topic for further reading.

## Conclusions

The rapid advancement from nascent technology to universal adoption of OCT in the clinic is a remarkable achievement. It highlights the importance of the information obtained from OCT imaging for modern ophthalmology clinical practice. The *in vivo* cross-sectional SD-OCT images of the macula provide detailed information regarding the various layers of the retina and allow quantitation of retinal thickness and volume. Wider field OCT images possible using SS-OCT allow peripheral pathology to be evaluated. Further development of OCT technology has resulted in OCTA, a rapid, noninvasive imaging method for visualizing retinal and choroidal vascular flow in 3D. iOCT imaging now guides surgical maneuvers and outcomes. Even functional information of the retina now can be obtained using OCT via ORG. Continued innovation in this field may herald new scientific and clinical application of OCT technology that may only be imagined at the current time.

## Acknowledgments

None.

## Footnote

**Reporting Checklist:** The authors have completed the Narrative Review reporting checklist. Available at <https://atm.amegroups.com/article/view/10.21037/atm-24-211/rc>

**Peer Review File:** Available at <https://atm.amegroups.com/article/view/10.21037/atm-24-211/prf>

**Funding:** This work was supported in part by the Barbara A. & Alan M. Roth, MD Endowed Chair for Discovery, Education and Patient Care in Visual Science (to S.S.P.) from the University of California Davis.

**Conflicts of Interest:** All authors have completed the ICMJE uniform disclosure form (available at <https://atm.amegroups.com/article/view/10.21037/atm-24-211/coif>).

S.S.P. serves as an unpaid editorial board member of *Annals of Translational Medicine* from October 2023 to September 2025. S.S.P. reports that this research was supported in part by the Barbara A. & Alan M. Roth, MD Endowed Chair for Discovery, Education and Patient Care in Visual Science (to S.S.P.) from the University of California Davis. S.S.P. received research grants from industries (EyePoint, Ophthea, Roche/Novartis) via employer to conduct clinical research evaluating intravitreal injection of drugs that inhibit vascular endothelial growth factor. S.S.P. has received honoraria from National Eye Institute and Department of Defense for grant reviews and from Boston University for invited lectures. S.S.P. also served as an unpaid grant reviewer for Retina Society as a member of the Research Committee. The other authors have no conflicts of interest to declare.

**Ethical Statement:** The authors are accountable for all aspects of the work in ensuring that questions related to the accuracy or integrity of any part of the work are appropriately investigated and resolved.

**Open Access Statement:** This is an Open Access article distributed in accordance with the Creative Commons Attribution-NonCommercial-NoDerivs 4.0 International License (CC BY-NC-ND 4.0), which permits the non-commercial replication and distribution of the article with the strict proviso that no changes or edits are made and the original work is properly cited (including links to both the formal publication through the relevant DOI and the license). See: <https://creativecommons.org/licenses/by-nc-nd/4.0/>.

## References

1. Nguyen KH, Patel BC, Tadi P. Anatomy, Head and Neck: Eye Retina. In: StatPearls [Internet]. StatPearls Publishing; 2023. Accessed February 19, 2024. Available online: <https://www.ncbi.nlm.nih.gov/books/NBK542332/>
2. Boulton M, Dayhaw-Barker P. The role of the retinal pigment epithelium: topographical variation and ageing changes. *Eye (Lond)* 2001;15:384-9.
3. Dowling JE. The Retina: An Approachable Part of the Brain. Cambridge: Harvard University Press; 2012. doi: 10.2307/j.ctv31zqj2d.
4. Molday RS, Moritz OL. Photoreceptors at a glance. *J Cell Sci* 2015;128:4039-45.
5. Narayan DS, Chidlow G, Wood JP, et al. Glucose



- metabolism in mammalian photoreceptor inner and outer segments. *Clin Exp Ophthalmol* 2017;45:730-41.
6. Omri S, Omri B, Savoldelli M, et al. The outer limiting membrane (OLM) revisited: clinical implications. *Clin Ophthalmol* 2010;4:183-95.
  7. Euler T, Haverkamp S, Schubert T, et al. Retinal bipolar cells: elementary building blocks of vision. *Nat Rev Neurosci* 2014;15:507-19.
  8. Masland RH. The neuronal organization of the retina. *Neuron* 2012;76:266-80.
  9. Kolb H. Inner Plexiform Layer. In: Kolb H, Fernandez E, Nelson R, eds. *Webvision: The Organization of the Retina and Visual System*. University of Utah Health Sciences Center; 1995. Accessed February 19, 2024. Available online: <http://www.ncbi.nlm.nih.gov/books/NBK11536/>
  10. Purves D, Augustine GJ, Fitzpatrick D, et al. Central Projections of Retinal Ganglion Cells. In: *Neuroscience*. 2nd Edition. Sinauer Associates; 2001. Accessed February 19, 2024. Available online: <https://www.ncbi.nlm.nih.gov/books/NBK11145/>
  11. Heegaard S, Jensen OA, Prause JU. Structure and composition of the inner limiting membrane of the retina. SEM on frozen resin-cracked and enzyme-digested retinas of *Macaca mulatta*. *Graefes Arch Clin Exp Ophthalmol* 1986;24:355-60.
  12. Kolb H, Fernandez E, Jones B, et al. *Simple Anatomy of the Retina*. 1995.
  13. Purves D, Augustine GJ, Fitzpatrick D, et al. Anatomical Distribution of Rods and Cones. In: *Neuroscience*. 2nd Edition. Sinauer Associates; 2001. Accessed February 19, 2024. Available online: <https://www.ncbi.nlm.nih.gov/books/NBK10848/>
  14. Lamb TD. Why rods and cones? *Eye (Lond)* 2016;30:179-85.
  15. Cones. American Academy of Ophthalmology. Published December 19, 2018. Accessed February 19, 2024. Available online: <https://www.aao.org/eye-health/anatomy/cones>
  16. Straatsma BR, Landers MB, Kreiger AE. The ora serrata in the adult human eye. *Arch Ophthalmol* 1968;80:3-20.
  17. Rods. American Academy of Ophthalmology. Published December 19, 2018. Accessed February 19, 2024. Available online: <https://www.aao.org/eye-health/anatomy/rods>
  18. Kiel JW. Anatomy. In: *The Ocular Circulation*. Morgan & Claypool Life Sciences; 2010. Accessed February 19, 2024. Available online: <https://www.ncbi.nlm.nih.gov/books/NBK53329/>
  19. Gupta N, Motlagh M, Singh G. Anatomy, Head and Neck, Eye Arteries. 2025. In: StatPearls. Treasure Island (FL): StatPearls Publishing; July 24, 2023.
  20. Nickla DL, Wallman J. The multifunctional choroid. *Prog Retin Eye Res* 2010;29:144-68.
  21. Huang D, Swanson EA, Lin CP, et al. Optical coherence tomography. *Science* 1991;254:1178-81.
  22. Zhang H, Salo D, Kim DM, et al. Penetration depth of photons in biological tissues from hyperspectral imaging in shortwave infrared in transmission and reflection geometries. *J Biomed Opt* 2016;21:126006.
  23. Fercher AF, Hitzenberger CK, Kamp G, et al. Measurement of intraocular distances by backscattering spectral interferometry. *Optics Communications* 1995;117:43-8.
  24. Bille JFA, Aumann S, Donner S, et al. *Optical Coherence Tomography (OCT): Principle and Technical Realization*. 2019.
  25. Kang SW, Park CY, Ham DI. The correlation between fluorescein angiographic and optical coherence tomographic features in clinically significant diabetic macular edema. *Am J Ophthalmol* 2004;137:313-22.
  26. Gabriele ML, Wollstein G, Ishikawa H, et al. Three dimensional optical coherence tomography imaging: advantages and advances. *Prog Retin Eye Res* 2010;29:556-79.
  27. Swanson EA, Izatt JA, Hee MR, et al. In vivo retinal imaging by optical coherence tomography. *Opt Lett* 1993;18:1864-6.
  28. Wojtkowski M, Bajraszewski T, Gorczyńska I, et al. Ophthalmic imaging by spectral optical coherence tomography. *Am J Ophthalmol* 2004;138:412-9.
  29. Puliafito CA, Hee MR, Lin CP, et al. Imaging of macular diseases with optical coherence tomography. *Ophthalmology* 1995;102:217-29.
  30. Yun S, Tearney G, Bouma B, et al. High-speed spectral-domain optical coherence tomography at 1.3  $\mu\text{m}$  wavelength. *Opt Express* 2003;11:3598-604.
  31. Heidelberg Engineering GmbH. *Spectralis HRA+OCT Hardware Operating Instructions*; 2007. Available online: [https://cdn.ymaws.com/www.opsweb.org/resource/collection/8C09696C-D8CA-4647-A6BF-B0B83369CA24/Spectralis\\_Hardware\\_Operating\\_Manual.pdf](https://cdn.ymaws.com/www.opsweb.org/resource/collection/8C09696C-D8CA-4647-A6BF-B0B83369CA24/Spectralis_Hardware_Operating_Manual.pdf)
  32. Carl Zeiss Meditec, Inc. *Cirrus HD-OCT User Manual*. 2019. Available online: <https://www.manualslib.com/manual/1566630/Zeiss-Cirrus-Hd-Oct-500.html>
  33. Alam S, Zawadzki RJ, Choi S, et al. Clinical application of rapid serial fourier-domain optical coherence tomography for macular imaging. *Ophthalmology* 2006;113:1425-31.

34. Carl Zeiss Meditec, Inc. Stratus OCT User Manual. 2010. Available online: <https://www.manualslib.com/manual/1288817/Zeiss-3000.html>
35. Drexler W, Morgner U, Ghanta RK, et al. Ultrahigh-resolution ophthalmic optical coherence tomography. *Nat Med* 2001;7:502-7.
36. Drexler W, Morgner U, Kärtner FX, et al. In vivo ultrahigh-resolution optical coherence tomography. *Opt Lett* 1999;24:1221-3.
37. Boppart SA, Bouma BE, Pitris C, et al. In vivo cellular optical coherence tomography imaging. *Nat Med* 1998;4:861-5.
38. Choma M, Sarunic M, Yang C, et al. Sensitivity advantage of swept source and Fourier domain optical coherence tomography. *Opt Express* 2003;11:2183-9.
39. Klein T, Huber R. High-speed OCT light sources and systems [Invited]. *Biomed Opt Express*. 2017;8:828-59.
40. Jia Y, Bailey ST, Hwang TS, et al. Quantitative optical coherence tomography angiography of vascular abnormalities in the living human eye. *Proc Natl Acad Sci U S A* 2015;112:E2395-402.
41. Li D, Li T, Paschalis EI, et al. Optic Nerve Head Characteristics in Chronic Angle Closure Glaucoma Detected by Swept-Source OCT. *Curr Eye Res* 2017;42:1450-7.
42. McNabb RP, Grewal DS, Mehta R, et al. Wide field of view swept-source optical coherence tomography for peripheral retinal disease. *Br J Ophthalmol* 2016;100:1377-82.
43. Litts KM, Ach T, Hammack KM, et al. Quantitative Analysis of Outer Retinal Tubulation in Age-Related Macular Degeneration From Spectral-Domain Optical Coherence Tomography and Histology. *Invest Ophthalmol Vis Sci* 2016;57:2647-56.
44. Cuenca N, Ortuño-Lizarán I, Pinilla I. Cellular Characterization of OCT and Outer Retinal Bands Using Specific Immunohistochemistry Markers and Clinical Implications. *Ophthalmology* 2018;125:407-22.
45. Jonnal RS, Kocaoglu OP, Zawadzki RJ, et al. The cellular origins of the outer retinal bands in optical coherence tomography images. *Invest Ophthalmol Vis Sci* 2014;55:7904-18.
46. Spaide RF, Curcio CA. Anatomical correlates to the bands seen in the outer retina by optical coherence tomography: literature review and model. *Retina* 2011;31:1609-19.
47. Park SS, Zawadzki RJ, Choi SS, et al. Maculopathy diagnosed with high-resolution fourier-domain optical coherence tomography in eyes with previously unexplained visual loss. *Retin Cases Brief Rep* 2010;4:233-9.
48. Park SS, Truong SN, Zawadzki RJ, et al. High-resolution Fourier-domain optical coherence tomography of choroidal neovascular membranes associated with age-related macular degeneration. *Invest Ophthalmol Vis Sci* 2010;51:4200-6.
49. Watson GM, Keltner JL, Chin EK, et al. Comparison of retinal nerve fiber layer and central macular thickness measurements among five different optical coherence tomography instruments in patients with multiple sclerosis and optic neuritis. *J Neuroophthalmol* 2011;31:110-6.
50. Chin EK, Sedeek RW, Li Y, et al. Reproducibility of macular thickness measurement among five OCT instruments: effects of image resolution, image registration, and eye tracking. *Ophthalmic Surg Lasers Imaging* 2012;43:97-108.
51. CAT'T Research Group; Martin DF, Maguire MG, et al. Ranibizumab and bevacizumab for neovascular age-related macular degeneration. *N Engl J Med* 2011;364:1897-908.
52. Fung AE, Lalwani GA, Rosenfeld PJ, et al. An optical coherence tomography-guided, variable dosing regimen with intravitreal ranibizumab (Lucentis) for neovascular age-related macular degeneration. *Am J Ophthalmol* 2007;143:566-83.
53. DeCroos FC, Reed D, Adam MK, et al. Treat-and-Extend Therapy Using Aflibercept for Neovascular Age-related Macular Degeneration: A Prospective Clinical Trial. *Am J Ophthalmol* 2017;180:142-50.
54. Brown DM, Schmidt-Erfurth U, Do DV, et al. Intravitreal Aflibercept for Diabetic Macular Edema: 100-Week Results From the VISTA and VIVID Studies. *Ophthalmology* 2015;122:2044-52.
55. Amoaku WM, Ghanchi F, Bailey C, et al. Diabetic retinopathy and diabetic macular oedema pathways and management: UK Consensus Working Group. *Eye (Lond)* 2020;34:1-51.
56. Pilli S, Lim P, Zawadzki RJ, et al. Fourier-domain optical coherence tomography of eyes with idiopathic epiretinal membrane: correlation between macular morphology and visual function. *Eye (Lond)* 2011;25:775-83.
57. Guymer RH, Rosenfeld PJ, Curcio CA, et al. Incomplete Retinal Pigment Epithelial and Outer Retinal Atrophy in Age-Related Macular Degeneration: Classification of Atrophy Meeting Report 4. *Ophthalmology* 2020;127:394-409.
58. Spaide RF, Koizumi H, Pozzoni MC. Enhanced depth imaging spectral-domain optical coherence tomography. *Am J Ophthalmol* 2008;146:496-500.

59. Cheung CMG, Lee WK, Koizumi H, et al. Pachychoroid disease. *Eye (Lond)* 2019;33:14-33.
60. Fingler J, Zawadzki RJ, Werner JS, et al. Volumetric microvascular imaging of human retina using optical coherence tomography with a novel motion contrast technique. *Opt Express* 2009;17:22190-200.
61. Schwartz DM, Fingler J, Kim DY, et al. Phase-variance optical coherence tomography: a technique for noninvasive angiography. *Ophthalmology* 2014;121:180-7.
62. Chin EK, Kim DY, Hunter AA 3rd, et al. Staging of macular telangiectasia: power-Doppler optical coherence tomography and macular pigment optical density. *Invest Ophthalmol Vis Sci* 2013;54:4459-70.
63. Szpernal J, Gaffney M, Linderman RE, et al. Assessing the Sensitivity of OCT-A Retinal Vasculature Metrics. *Transl Vis Sci Technol* 2023;12:2.
64. Andrade Romo JS, Linderman RE, Pinhas A, et al. Novel Development of Parafoveal Capillary Density Deviation Mapping using an Age-Group and Eccentricity Matched Normative OCT Angiography Database. *Transl Vis Sci Technol* 2019;8:1.
65. Mo S, Krawitz B, Efstathiadis E, et al. Imaging Foveal Microvasculature: Optical Coherence Tomography Angiography Versus Adaptive Optics Scanning Light Ophthalmoscope Fluorescein Angiography. *Invest Ophthalmol Vis Sci* 2016;57:OCT130-40.
66. Mukkamala L, Nguyen M, Chang M, et al. Repeatability of Vascular Density Measurement of the Three Retinal Plexus Layers Using OCT Angiography in Pathologic Eyes (OCTA Vascular Density Repeatability of Three Plexus Layers). *Clin Ophthalmol* 2021;15:93-103.
67. Linderman R, Salmon AE, Strampe M, et al. Assessing the Accuracy of Foveal Avascular Zone Measurements Using Optical Coherence Tomography Angiography: Segmentation and Scaling. *Transl Vis Sci Technol* 2017;6:16.
68. Buffolino NJ, Vu AE, Amin A, et al. Factors Affecting Repeatability of Foveal Avascular Zone Measurement Using Optical Coherence Tomography Angiography in Pathologic Eyes. *Clin Ophthalmol* 2020;14:1025-33.
69. Dansingani KK, Inoue M, Engelbert M, et al. Optical coherence tomographic angiography shows reduced deep capillary flow in paracentral acute middle maculopathy. *Eye (Lond)* 2015;29:1620-4.
70. Kwan CC, Fawzi AA. Imaging and Biomarkers in Diabetic Macular Edema and Diabetic Retinopathy. *Curr Diab Rep* 2019;19:95.
71. Decker NL, Duffy BV, Boughanem GO, et al. Macular Perfusion Deficits on OCT Angiography Correlate with Nonperfusion on Ultrawide-field Fluorescein Angiography in Diabetic Retinopathy. *Ophthalmol Retina* 2023;7:692-702.
72. Pan J, Chen D, Yang X, et al. Characteristics of Neovascularization in Early Stages of Proliferative Diabetic Retinopathy by Optical Coherence Tomography Angiography. *Am J Ophthalmol* 2018;192:146-56.
73. McClintic SM, Kim DY, Fingler J, et al. Detection of pigment epithelial detachment vascularization in age-related macular degeneration using phase-variance OCT angiography. *Clin Ophthalmol* 2015;9:1299-305.
74. Kim DY, Fingler J, Zawadzki RJ, et al. Optical imaging of the chorioretinal vasculature in the living human eye. *Proc Natl Acad Sci U S A* 2013;110:14354-9.
75. Park SS, Thinda S, Kim DY, et al. Phase-Variance Optical Coherence Tomographic Angiography Imaging of Choroidal Perfusion Changes Associated With Acute Posterior Multifocal Placoid Pigment Epitheliopathy. *JAMA Ophthalmol* 2016;134:943-5.
76. Spaide RF, Fujimoto JG, Waheed NK. IMAGE ARTIFACTS IN OPTICAL COHERENCE TOMOGRAPHY ANGIOGRAPHY. *Retina* 2015;35:2163-80.
77. Zhang Q, Zhang A, Lee CS, et al. Projection artifact removal improves visualization and quantitation of macular neovascularization imaged by optical coherence tomography angiography. *Ophthalmol Retina* 2017;1:124-36.
78. Hormel TT, Huang D, Jia Y. Artifacts and artifact removal in optical coherence tomographic angiography. *Quant Imaging Med Surg* 2021;11:1120-33.
79. Jiang H, Simms AG, Sadaghiani S, et al. Multi-Center Repeatability of Macular Capillary Perfusion Density Using Optical Coherence Tomography Angiography. *Clin Ophthalmol* 2022;16:3069-78.
80. Mukkamala LK, Avaylon J, Welch RJ, et al. Intraoperative Retinal Changes May Predict Surgical Outcomes After Epiretinal Membrane Peeling. *Transl Vis Sci Technol* 2021;10:36.
81. Inoue M, Itoh Y, Koto T, et al. Intraoperative OCT Findings May Predict Postoperative Visual Outcome in Eyes with Idiopathic Macular Hole. *Ophthalmol Retina* 2019;3:962-70.
82. Ehlers JP, Tao YK, Srivastava SK. The value of intraoperative optical coherence tomography imaging in vitreoretinal surgery. *Curr Opin Ophthalmol* 2014;25:221-7.

83. Park SS, Bauer G, Abedi M, et al. Intravitreal autologous bone marrow CD34+ cell therapy for ischemic and degenerative retinal disorders: preliminary phase 1 clinical trial findings. *Invest Ophthalmol Vis Sci* 2014;56:81-9.
84. Liu Z, Kurokawa K, Zhang F, et al. Imaging and quantifying ganglion cells and other transparent neurons in the living human retina. *Proc Natl Acad Sci U S A* 2017;114:12803-8.
85. Soltanian-Zadeh S, Kurokawa K, Liu Z, et al. Weakly supervised individual ganglion cell segmentation from adaptive optics OCT images for glaucomatous damage assessment. *Optica* 2021;8:642-51.
86. Warner RL, Brainard DH, Morgan JIW. Repeatability and reciprocity of the cone optoretinogram. *Biomed Opt Express* 2022;13:6561-73.
87. Vienola KV, Valente D, Zawadzki RJ, et al. Velocity-based optoretinography for clinical applications. *Optica* 2022;9:1100-8.
88. Mariottoni EB, Datta S, Shigueoka LS, et al. Deep Learning-Assisted Detection of Glaucoma Progression in Spectral-Domain OCT. *Ophthalmol Glaucoma* 2023;6:228-38.
89. Subramaniam MD, Aishwarya Janaki P, Abishek Kumar B, et al. Retinal Changes in Parkinson's Disease: A Non-invasive Biomarker for Early Diagnosis. *Cell Mol Neurobiol* 2023;43:3983-96.
90. Curro KR, van Nispen RMA, den Braber A, et al. Longitudinal Assessment of Retinal Microvasculature in Preclinical Alzheimer's Disease. *Invest Ophthalmol Vis Sci* 2024;65:2.
91. Snyder PJ, Alber J, Alt C, et al. Retinal imaging in Alzheimer's and neurodegenerative diseases. *Alzheimers Dement* 2021;17:103-11.

**Cite this article as:** Langlo CS, Amin A, Park SS. Optical coherence tomography retinal imaging: narrative review of technological advancements and clinical applications. *Ann Transl Med* 2025;13(2):17. doi: 10.21037/atm-24-211